Polymer Bulletin 59, 685–697 (2007)
DOI 10.1007/s00289-007-0798-1

Polymer Bulletin

Non-isothermal Crystallization Kinetics of Poly (Ethylene Terephthalate)/Grafted Carbon Black Composite

Xianhui Li, Weihong Guo, Qilin Zhou, Shiai Xu, Chifei Wu (✉)

Polymer Alloy Laboratory, School of Materials Science and Engineering, East China University of Science and Technology, Shanghai 200237, People's Republic of China
E-mail: wucf@ecust.edu.cn; Fax: +86-21-64252569

Received: 7 February 2007 / Revised version: 25 April 2007 / Accepted: 4 June 2007
Published online: 15 June 2007 –

Summary

The grafted carbon black (GCB) was prepared by *in-situ* grafting low molecular weight compound on the surface of carbon black (CB) using a new technique. Poly(ethylene terephthalate)/grafted carbon black (PET/GCB) and poly(ethylene terephthalate)/ carbon black (PET/CB) composites were prepared by melt blending. The non-isothermal crystallization process of virgin Poly(ethylene terephthalate) (PET), PET/CB, and PET/GCB composites were investigated by differential scanning calorimetry (DSC), and the non-isothermal crystallization kinetics was analyzed using different approaches, i.e. modified Avrami equation, Ozawa equation and the method developed by Liu. The effective energy barrier ΔE of virgin PET, PET/CB, and PET/GCB composites were calculated using the differential iso-conversional method. All of the results showed that GCB and CB acted as nucleating agents and increased the crystallization rate of PET. Compared with CB, GCB was a more effective nucleator for PET.

Introduction

Poly(ethylene terephthalate) (PET) is a semi-crystalline polymer with high performance and low cost, which is widely used in many areas, including fibers, packaging films, bottles for beverage, and engineering components [1]. However, its applications are limited to high speed processing such as injection molding, due to the slow crystallization rate. This problem can be solved by adding nucleating agents, such as inorganic fillers [2-9] and organic carboxylic acid salts [10].

Carbon black (CB) has been widely used as polymer additives, for example reinforcing fillers, pigments and electrically conductive additives etc [11-13]. Over the last decade, numerous studies have been carried out on CB-filled polymers, for example electrical conductivity [14, 15] and the positive temperature coefficient (PTC) phenomenon [16–20]. After adding to semi-crystalline polymers, it was found that CB had tremendous influence on crystallization of the polymeric matrix [21], acting as nucleating agent and increasing the crystallization rate. This behavior has been observed for polypropylene (PP)/CB composite [22-23], polyvinylidene fluoride (PVDF)/CB composite, and polyamide (PA)/CB composite [24]. CB was also added into poly (ethylene terephthalate) (PET) [25-26], and the addition of CB could impact

on the properties of PET inevitably, especially on the crystallization behaviors. However, effects of CB on the crystallization of PET and the non-isothermal crystallization kinetics of PET/CB were seldom reported.
Recently, a new technique was proposed to graft CB with low molecular weight compound by *in-situ* reaction in our laboratory [27]. The aggregates of CB were broken by strong shearing in the process of grafting, and at the same time low molecular weight compound was *in-situ* grafted on the surface of CB particles, preventing their congregation. The grafted carbon black particles (GCB) with smaller size were obtained. Moreover, the GCB could be dispersed in polymer or organic solvent stably and uniformly [27]. Given the promising dispersion and properties achieved with the grafted carbon black (GCB) composite, it is desired to understand its impact on the crystallization behavior of polymer matrix like PET.
In this paper, the non-isothermal crystallization kinetics of PET filled with GCB and CB was investigated, and particular attention was placed on the nucleation of GCB on the crystallization of the matrix.

Experimental

Materials

The PET pellets used in this study were purchased from Yizheng Chemical Fibre Co., Ltd. (Yizheng, China). The intrinsic viscosity of PET in a mixture solvent of phenol/tetrachloroethane (60/40 wt/wt) at 30°C is 0.612 dL/g. The CB (furnace CB, N220) was kindly supplied by Cabot Company (USA). The untreated CB had a primary particle size of 25nm, di-n-butyl phthalate(DBP) absorption value (ASTM D2414) of 114 ml/100g, cetyl trimethyl ammonium bromide (CTAB)(ASTM D3765) of 108 m^2/g, iodine number (ASTM D1510) of 121mg/g. The low molecular weight compound that grafted on CB was 3,9-bis-[1,1-dimethyl-2{-(3-tert-butyl-4-hydroxyl-5-methylphenyl) propionyloxy}ethyl]-2,4,8,10-tertaoxaspiro-[5,5]-undne (AO-80), a commercial antioxidant for polymer(ADK STAB AO-80) supplied by Asahi Denka Industries Co. (Japan), and the molecular structure was shown in Figure 1.

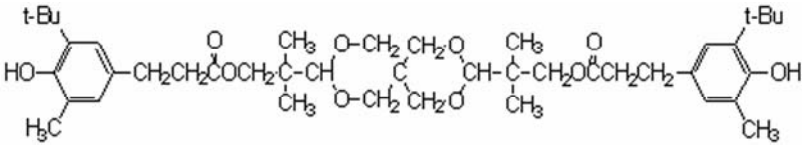

Figure 1 Chemical structure of AO-80

Sample preparation

The grafted carbon black was prepared in an internal batch mixer (Haake Rheomix600p, German), operating at 140°C and a rotor speed of 60 rpm according to the patent [27]. CB and AO-80 were pre-mixed at 1/0.8 (wt/wt) ratios, and was then added into the mixer and blended for about 30min under strong shearing. The mixture was washed and filtered for three times using acetone and then was extracted using acetone for 72h to remove any free AO-80. After that, the GCB was detected by thermogravimetry analysis (TGA) and grafting ratio of AO-80 was about 8.4% [27].

The PET/GCB and PET/CB composites containing 3 wt% GCB or CB were prepared via melt blending in a torque rheometer (Haake Rheomix3000p, German) at 265°C. The PET resin, GCB, and CB were dried at 120°C in a vacuum oven for 10h before processing. The PET was added into chamber of the rheometer to melt, and after about 2 min, the 3wt % CB or GCB was added and blended for another 6 min. The PET/GCB and PET/CB composites were obtained. A control sample was also prepared by processing virgin PET through the same procedures.

Scanning Electron Microscopy (SEM)

PET/CB and PET/GCB composites were made into flat discs by complete melting at 290°C on a hot stage followed by compression. They were then cooled and broken in liquid nitrogen. The broken sections of the two samples were coated with gold and then observed in a JEOL JSM-5410 scanning electron microscope (Tokyo, Japan) with a working voltage of 15kV.

Differential Scanning Calorimetry (DSC) measurements

The DSC measurements were carried out on NETZSCH DSC 200 PC. The temperature was calibrated using a high-purity indium, with a melting point of 156.4°C and a fusion enthalpy of 28.40J/g. The sample weight was about 5.2 to 5.7 mg. All the samples were dried in a vacuum oven at 60°C for 6 h before testing. The measurements were carried out in nitrogen atmosphere. The sample was initially heated to 290°C, and held for 8 min in order to remove prior thermal history. Then it was cooled to 80°C at 2.5, 5, 10, and 20°C /min, respectively. The crystallization parameters, the temperature at the exothermal peak (T_c) and the temperature of the onset of crystallization (T_o), were obtained from the cooling scans.

Results and discussion

Dispersibilities of CB and GCB in PET

Figure 2 showed the broken sections of PET/CB and PET/GCB observed by SEM. It can be seen that CB and GCB were dispersed well in PET under the blending

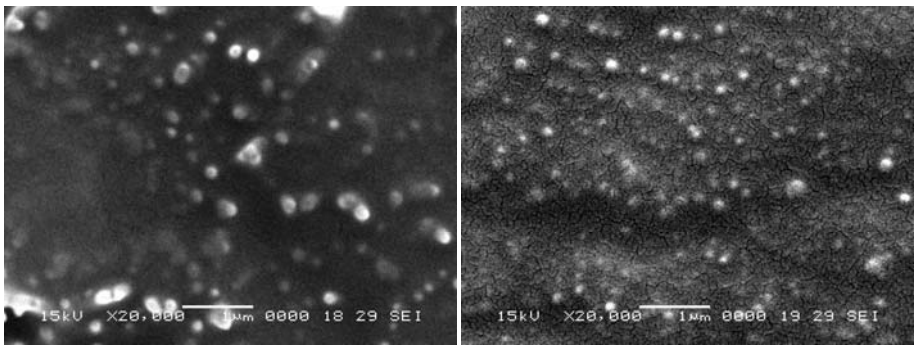

a) PET/CB b) PET/GCB

Figure 2 SEM photos of PET/CB and PET/GCB

conditions used in this paper. In addition, GCB was dispersed more uniformly, and its particles were smaller in PET, compared with CB. This phenomenon results from the preparing process of GCB. It is known that the primary particles of CB fuse together to form aggregates, which are usually considered as the primary structure of CB [28]. Those aggregates of CB can be broken by the shear force during mechanical blending and the *in-situ* grafted AO-80 can stabilize the broken aggregates, result in smaller CB particles [27]. Therefore, GCB exhibited more uniform and smaller particles than CB when dispersed into PET.

Non-isothermal crystallization process

The non-isothermal crystallization processes of PET, PET/CB, and PET/GCB composites from the melt were measured at various cooling rates from 2.5 to 20°C/min. The DSC curves of all the samples are presented in Figure 3a).

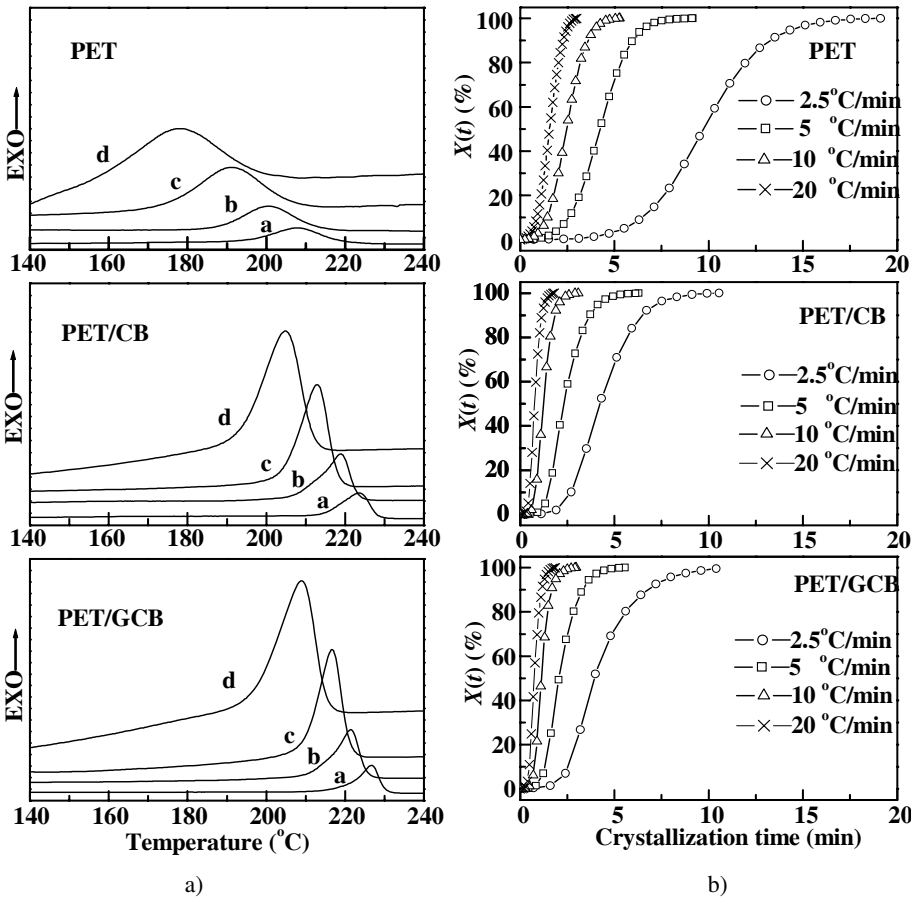

a) b)

Figure 3 a) DSC curves of virgin PET, PET/CB, and PET/GCB in the crystallization process from the melt at various cooling rate: a, 2.5°C/min; b, 5°C/min; c, 10°C/min; d, 20°C/min; b) Plots of $X(t)$ versus crystallization time at different cooling rates at different cooling rates

For PET, as cooling from 290°C at various rates, all the curves reveal a single exothermal crystallization peak. The peak becomes broader and shifts to lower temperature as the cooling rate increases. A similar trend is observed for the PET/CB and PET/GCB composites. The crystallization parameters, T_c and T_o, are listed in Table 1. As shown, the T_c and T_o values of PET/CB and PET/GCB composites are higher than those of the PET at the same cooling rate. Obviously, crystallization of the composites can be conducted at higher temperature compared with the virgin PET. The observed increase of T_c with addition of CB and GCB is typical characteristics of nucleation-controlled crystallization [29]. This implies that CB and GCB in the composites act as nucleating agent during the crystallization of the PET matrix. The T_c of PET/GCB composite is higher than that of the PET/CB composite at a given cooling rate. For example at the cooling rate of 10°C/min, T_c is 212.9°C for the PET/CB composite and 216.7°C for the PET/GCB composite. This suggests that GCB is a more effective nucleator for PET.

In the non-isothermal crystallization process, the relative crystallinity $X(T)$, a function of crystallization temperature T, can be formulated as

$$X(T) = \int_{T_o}^{T} (\frac{dH_c}{dT})dT \Big/ \int_{T_o}^{T_\infty} (\frac{dH_c}{dT})dT \quad (1)$$

where T_o and T_∞ represent the temperatures at the onset and the end of the crystallization process, respectively, and dH_c is the enthalpy of the crystallization released during an infinitesimal temperature range dT [30]. The crystallization time (t) can be calculated by the following:

$$t = (T_o - T) / |\beta| \quad (2)$$

where T is the temperature at time t, and β is the cooling rate.

Table 1 Crystallization parameters of virgin PET, PET/CB, and PET/GCB composites

	β(°C/min)	T_o(°C)	T_c(°C)	$t_{1/2}$(min)
PET	2.5	230.6	208.0	9.73
	5	221.6	200.6	4.24
	10	215.4	191.3	2.47
	20	208.6	178.0	1.56
PET/CB	2.5	232.8	223.5	4.23
	5	228.6	218.8	2.31
	10	224.0	212.9	1.23
	20	218.6	204.7	0.77
PET/GCB	2.5	235.0	226.7	3.93
	5	230.2	221.4	2.05
	10	227.0	216.7	1.13
	20	221.8	208.9	0.74

Figure 3b) shows the plots of the relative crystallinity $X(t)$ versus crystallization time t. From these curves, the half-time of crystallization ($t_{1/2}$), can be determined, as summarized in Table 1 for PET, PET/CB, and PET/GCB composites. As shown, $t_{1/2}$ decreases as increasing cooling rate. That indicates that the crystallization of the PET can be conducted fast at higher cooling rate. At the same cooling rate, $t_{1/2}$ for the three samples follows the order: $t_{1/2\ (PET)} > t_{1/2\ (PET/CB)} > t_{1/2\ (PET/GCB)}$. Clearly, the crystallization

rate of PET has been significantly accelerated after addition of CB or GCB. And GCB seems to be a much more efficient nucleating agent for PET compared with CB [7-9].
As discussed above, GCB has smaller particles than CB. Thus, with the same amount of GCB or CB added, the number of particles in the PET/GCB composite is much more than that in the PET/CB composite. Therefore, the number of heterogeneous nuclei in PET/GCB is more than that in PET/CB. At the same time, the AO-80 molecules grafted on the surface of CB can enhance the interaction between the PET and CB particles. The two factors result in that GCB has a higher nucleating activity than CB and can further accelerate the crystallization rate of PET.

Non-isothermal crystallization kinetics

For isothermal crystallization, the kinetics can be analyzed with the Avrami equation [31]

$$1 - X(t) = \exp(-Z t^{n}) \tag{3}$$

where $X(t)$, Z, and n denote the relative crystallinity at the time t, the crystallization rate constant and the Avrami exponent which describes the mechanism of crystallization, respectively. Equation (3) can be transformed to Equation (4).

$$\text{Log}[-\text{Ln}(1 - X(t))] = \text{Log}\, Z + n\, \text{Log}\, t \tag{4}$$

The Avrami equation was also used to analyze non-isothermal crystallizations [32]. Although, the physical meaning of Z and n cannot be directly related to a non-isothermal crystallization, they can provide further insight into the kinetics. Considering the non-isothermal character of the process investigated, the value of Z, should be adequately revised using the cooling rate, β, as the following

$$\text{Log}\, Z_c = (\text{Log}\, Z) / \beta \tag{5}$$

where Z_c is the revised crystallization rate constant.
Plotting Log[-Ln(1-$X(t)$)] versus Log t, a straight line should be obtained, Z and n correspond to the intercept and slope of the line respectively. Figure 4 displays the plots of Log[-Ln(1-$X(t)$)] versus Log t for PET, PET/CB, and PET/GCB composites at different cooling rates.
As shown in Figure 4, for all samples, there exist two stages of crystallization at a given cooling rate. The initial part (Log[-Ln(1-$X(t)$)] < 0) shows a linear relationship and Z and n can be calculated. At the late stage the curves deviate from the linear relationship suggesting secondary crystallization and spherulite impingement. Besides, the diffusion of polymer chains is restricted in the crystallite frontier by the heterogeneous particles in the PET/CB and PET/GCB composites. This may contribute to the deviation as well. Similar results were also observed in isotactic PP/CB [21], PET/clay [33], and nylon 6/foliated graphite [34].
n, Z, and Z_c for PET, PET/CB, and PET/GCB calculated from the linear parts (i.e. initial parts: Log[-Ln(1-$X(t)$)] < 0) are collected in Table 2. The values of n for virgin PET range from 3.15 to 4.31, indicating that the crystal growth is three-dimensional (spherulitic) with homogeneous nucleation. This agrees with the isothermal crystallization of PET observed by Wan and his coworkers [33]. For PET/CB and PET/GCB composites, n is between 4 and 5, larger than those of virgin PET. Similar phenomena also were observed in PET/disodium terephthalate (DST) [35], and PET/silica [36] in isothermal crystallization. This means that the mechanisms of the

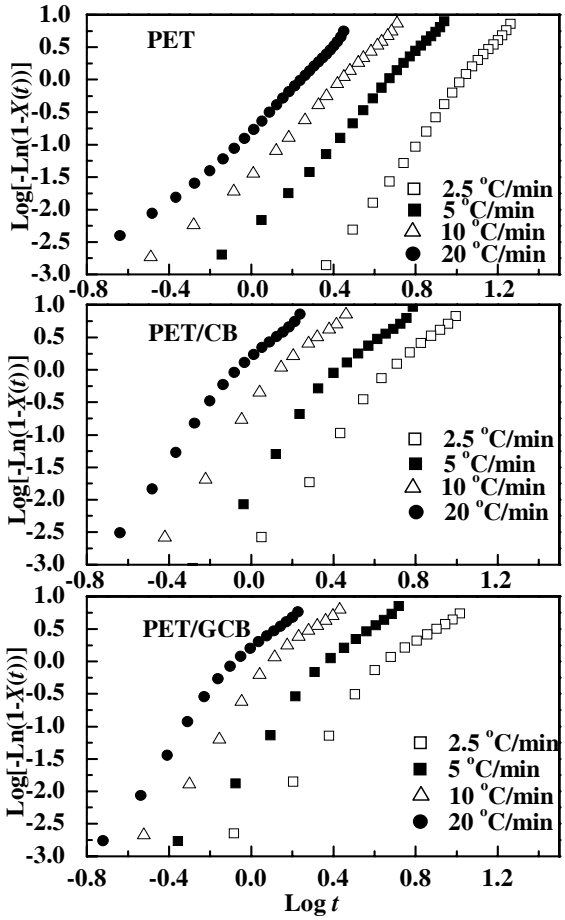

Figure 4 Plots of Log [-Ln(1-*X* (*t*))] versus Log *t*

Table 2 Results of the Avrami analysis for non-isothermal crystallization of virgin PET and its composites PET/CB and PET/GCB

	β (°C /min)	$Z\times10^3(s^{-n})$	Z_c	n
PET	2.5	0.037	0.017	4.31
	5	4.887	0.345	3.33
	10	36.922	0.719	3.15
	20	169.208	0.915	3.04
PET/CB	2.5	1.440	0.073	4.28
	5	15.221	0.433	4.53
	10	275.352	0.879	4.87
	20	2108.371	1.038	4.30
PET/GCB	2.5	1.754	0.079	4.39
	5	28.829	0.492	4.50
	10	356.505	0.902	4.42
	20	2917.757	1.055	4.66

non-isothermal crystallization of the PET/CB and PET/GCB are more complicated than PET. Clearly, CB and GCB can significantly influence the mechanism of nucleation and crystal growth of PET [35-37]. Moreover, based on the mode of evolution of PET spherulite revealed by Lee[38], Bian [35] proposed that n values relate with the number of growth points in crystal lamellae, namely, the bigger the number is, the larger the n values. Therefore, growth points in crystallization increase due to the addition of CB and GCB in PET, which results in larger values of n for PET/CB and PET/GCB.

Z and Z_c for PET/CB and PET/GCB are significantly higher than that of virgin PET at same cooling rate, suggesting a much higher crystallization rate for PET in the composites. Z and Z_c for PET/GCB are larger than that for PET/CB, i.e. the crystallization rate of PET/GCB is faster than that of PET/CB, in agreement with the results of $t_{1/2}$.

Another method to describe the nonisothermal crystallization kinetics was developed by Ozawa [39]. In this approach the relative crystallinity can be written as a function of cooling rate as Equation (6).

$$1 - X(T) = \exp[-P(T) / \beta^m] \tag{6}$$

The double-logarithmic form of Equation (6) is shown as following

$$\text{Log}[-\text{Ln}(1 - X(T))] = \text{Log}\, P(T) - m\, \text{Log}\, \beta \tag{7}$$

where $P(T)$ is the Ozawa crystallization rate constant, and m is the Ozawa exponent.

Consequently, plotting of Log[-Ln(1-$X(T)$)] against Log β at a fixed temperature should give a straight line if the Ozawa approach is valid. The Ozawa crystallization rate constant ($P(T)$) and Ozawa exponent (m) can be determined from the intercept, and the slope of the line, respectively. Log[-Ln(1-$X(T)$)] is plotted versus Log β for virgin PET, PET/CB, and PET/GCB at different temperatures in Figure 5. As shown, for virgin PET, there exists a linear relationship between Log[-Ln(1-$X(T)$)] and Log β, which suggests that the Ozawa approach is valid for PET here. The Ozawa exponents (m), calculated from the slop of the line, are 1.97, 2.22, 2.36, 2.52, 2.76, and 3.03 at 194, 198, 200, 202, 204, and 210°C, respectively. However, the Ozawa equation can't describe the process of their non-isothermal crystallization of PET/CB and PET/GCB composites satisfactorily as shown in Figure 5. Similar results were also reported for poly (etherether ketone) (PEEK) [40], poly (ether ketone ether ketone ketone) (PEKEKK) [41], and POM/MMT nanocomposites [42].

The Ozawa equation was derived from the Avrami theory, in which secondary crystallization and impingement of spherulites were ignored. But, as discussed above, for PET/CB and PET/GCB, secondary crystallization and impingement were significant [33]. In addition, the Ozawa equation described the overlapping parts of the crystallization peaks at different cooling rate. However, as shown in Figure 2, the overlapping portion of each crystallization peak is located at different crystallization for different cooling rates. Thus, the deviation from the Ozawa equation for the non-isothermal crystallization of PET/CB and PET/GCB may be due to the crystallization being in different periods for different cooling rates at a given temperature. For example, the crystallization is at the beginning stage for a higher cooling rate, and at the late stage for a lower cooling rate,where secondary crystallization exists. This phenomenon is more evident when the difference of β is large [43].

Combining the Avrami equation and the Ozawa equation, a new approach was developed by Liu et al [40] to describe the kinetics of non-isothermal crystallization.

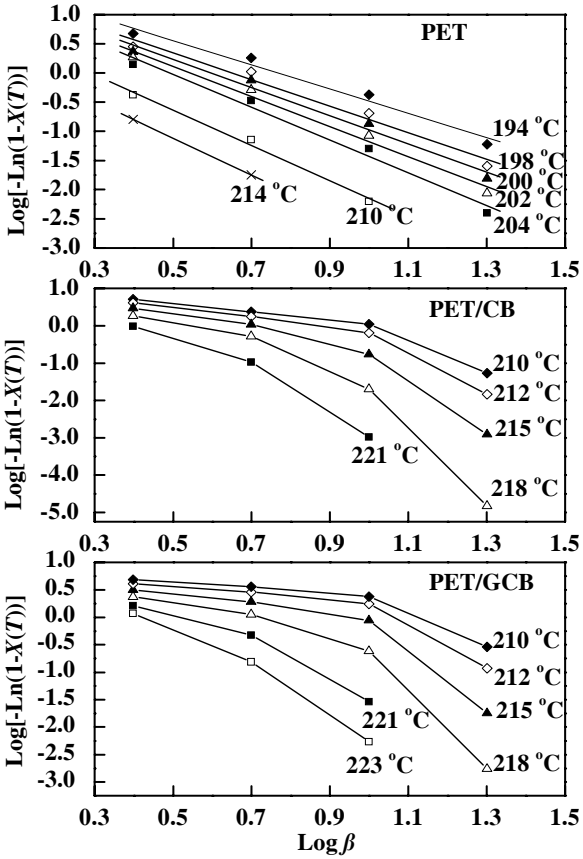

Figure 5 Plots of Log[- Ln(1 - $X(T)$)] versus Log β for PET, PET/CB, and PET/GCB

For a given non-isothermal crystallization process, comparing Equation (4) and (7), the following equation is obtained [40].

$$\text{Log } Z + n \text{ Log } t = \text{Log } P(T) - m \text{ Log } \beta \tag{8}$$

After rearrangement, the final form is achieved

$$\text{Log } \beta = \text{Log } F(T) - a \text{ Log } t \tag{9}$$

here, $F(T)(=[P\ (T)/Z]^{1/m})$ is the kinetics parameter, referring to the value of cooling rate that has to be chosen at the unit crystallization time when the measured system amounts to a certain degree of crystallinity, and α is the ratio of the Avrami exponent n to the Ozawa exponent m (i.e., $\alpha = n/m$).

For non-isothermal crystallization at different cooling rate, plotting Log β against Log t at a given relative crystallinity, should give a straight line. The values of α and $F(T)$ can be determined from the slope and intercept of the line, respectively. The plots of Log β versus Log t for virgin PET, PET/CB, and PET/GCB at different relative crystallinity are shown in Figure 6. Clearly, the Liu approach can well describe the non-isothermal crystallization for all of them.

$F(T)$ and α, achieved from the intercept and the slope in Figure 6, respectively, are summarized in Table 3. For a given sample, α is almost constant, while $F(T)$ increases

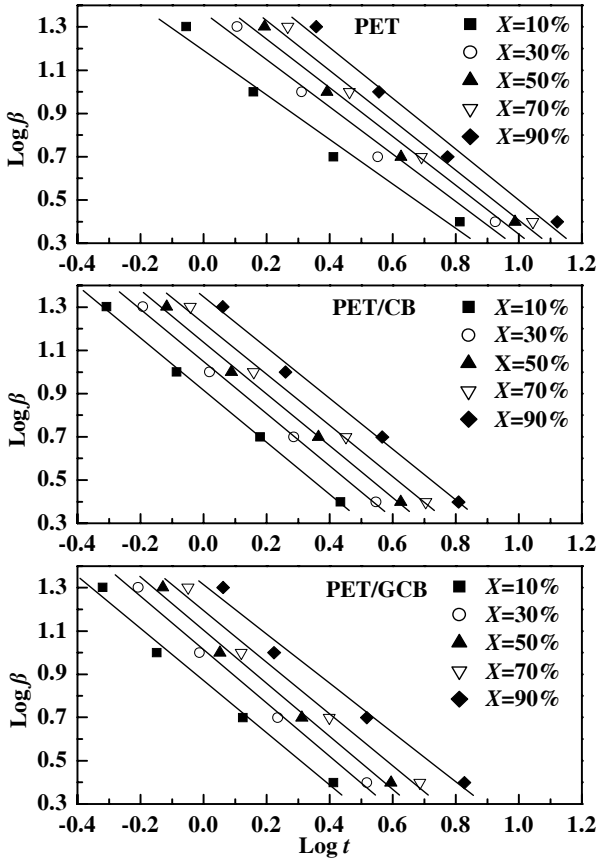

Figure 6 Plots of Log β versus Log t for virgin PET, PET/CB, and PET/GCB at different relative crystallinity

with the relative crystallinity increasing. This suggests higher cooling rate should be used to obtain a higher degree of relative crystallinity at unit crystallization time. For the same relative crystallinity, the $F(T)$ of PET is the highest, and that of PET/GCB is the lowest, which means that the crystallization rate of PET/GCB is fastest, in well agreement with the statement made from the Avrami equation and $t_{1/2}$.

Table 3 Non-isothermal crystallization kinetic parameters at different relative degrees of crystallinity by Liu method

		X (%)				
		10	30	50	70	90
PET	$F(T)$	15.56	23.32	29.48	36.36	47.40
	α	1.03	1.09	1.13	1.15	1.18
PET/CB	$F(T)$	8.25	11.19	13.73	16.83	22.26
	a	1.21	1.21	1.20	1.18	1.17
PET/GCB	$F(T)$	7.43	10.33	12.71	15.66	20.63
	a	1.21	1.23	1.23	1.12	1.14

Effective energy barrier

Usually, effective energy barrier, ΔE, of non-isothermal crystallization of polymer melts can be evaluated by the Kissinger equation [44]

$$d[\mathrm{Ln}(\beta/T_c^2)]/d(1/T_c) = -\Delta E/R \tag{10}$$

here, β and T_c stand for the cooling rate and the peak temperature, and R is the universal gas constant.

Recently, Vyazovkin [45] has demonstrated that dropping the negative sign for β is a mathematically invalid procedure that generally makes the Kissinger equation inapplicable to the processes that occur on cooling. The use of this invalid procedure may result in erroneous values of the effective energy barrier, ΔE.

Therefore, the differential iso-conversional method of Friedman [46] and the integral iso-conversional method of Vyazovkin [47] are appropriate for melt crystallization. In this work, the Friedman method will be used, mainly due to the reliability and simplicity of the method [47]. The Friedman equation is expressed as

$$\ln\left(\frac{dX}{dt}\right)_{X,i} = \text{constant} - \frac{\Delta E_X}{RT_{X,i}} \tag{11}$$

where dX/dt is the instantaneous crystallization rate as a function of time at a given conversion X, ΔE_X is the effective energy barrier at a given conversion X, $T_{X,i}$ is the set of temperatures related to a given conversion X at different cooling rates, and the subscript i refer to every individual cooling rate used.

According to this method, the $X(t)$ function obtained from the integration of the experimentally measured crystallization rates is initially differentiated with respect to time to obtain the instantaneous crystallization rate, dX/dt. Furthermore, by selecting appropriate degrees of crystallinity (i.e., from 5 to 95%) the values of dX/dt at a specific X are correlated to the corresponding crystallization temperature at this X, that is, T_X. Then, by plotting the left hand side of Equation (11) with respect to $1/T_X$, a straight line must be obtained with a slope equal to $\Delta E_X/R$. In this work, the correlation coefficients for every sample were in the range of 0.940 to 0.985.

Figure 7 shows the dependence of effective energy barrier ΔE on the extent of relative crystallization for virgin PET, PET/CB, and PET/GCB composites. For all of the

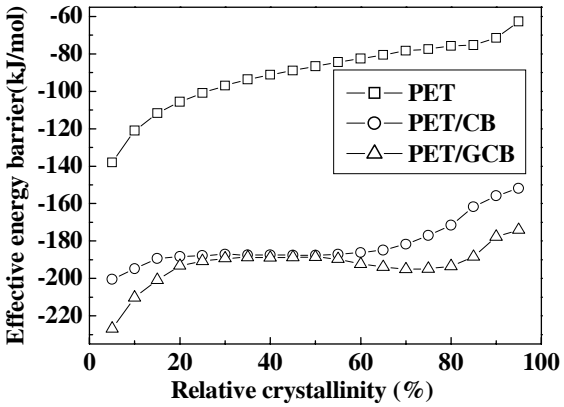

Figure 7 Dependence of the effective activation energy on the relative extent of crystallization for virgin PET, PET/CB, and PET/GCB composites

samples studied, ΔE is generally found to increase with increasing the extent of relative crystallization, suggesting that as the crystallization proceeded it was more difficult for each polymer system to crystallize. The ΔE values of PET/CB and PET/GCB composites are much lower than that of virgin PET at all extent of relative crystallization. And the ΔE value of PET/GCB is lower than that of PET/CB. It should be noted that the lower the ΔE value, the higher the crystallization ability of the polymer system [48]. Therefore this trend shows that CB and GCB dispersed in the composites act as a heterogeneous nucleation for the crystallization of PET and accelerate the crystallization process. The effect of GCB is stronger than that of CB.

Conclusion

The non-isothermal crystallization behaviors of virgin PET, PET/CB, and PET/GCB composites were investigated, and the non-isothermal crystallization kinetics was analyzed by different approaches, including the modified Avrami equation, the Ozawa equation and the Liu method. CB and GCB acted as nucleating agents for PET. Moreover, the nucleation ability of GCB was higher than that of CB because of smaller particle size and improved interaction between GCB and PET. The $t_{1/2}$ and crystallization rate constant suggested that the crystallization rate follows the order PET/GCB>PET/CB>PET. The method developed by Liu can well describe the non-isothermal crystallization of all the three samples. The values of $F(T)$ also showed that the crystallization rate of PET/GCB composite was the highest. The effective energy barrier ΔE of virgin PET, PET/CB and PET/GCB composites were calculated from the differential iso-conversional method of Friedman. It is concluded the values of ΔE of PET/CB and PET/GCB composites were lower than that of PET, meaning that crystallization of PET became easier after CB and GCB were introduced into PET. Therefore, all these results supported that CB and GCB acted as nucleating agents and increased the crystallization rate of PET, and GCB was an effective nucleator compared with CB.

Acknowledgements. Thanks for the financial assistance of National Nature Science Fundation of China (20574019).

References

1. Guo W, Tang X, Yin G, Gao Y, Wu C (2006) J Appl Polym Sci 102: 2692.
2. Ou C, Ho M, Lin J (2004) J Appl Polym Sci 91: 140.
3. Cheng S, Shank RA (1993) J Appl Polym Sci 47: 2149.
4. Run M, Wu S, Zhang D, Wu G (2005) Polymer 46: 5308.
5. Zhu P, Ma D (2000) Eur Polym J 36: 2471.
6. Dilorenzo ML, Errico ME, Avella M (2002) J Mater Sci 37: 2351.
7. Zhu Y, Li Z, Zhang D, Tanimoto T (2006) J Polym Sci Part B 44: 1351.
8. Ou C, Ho M, Lin J (2003) J Polym Res 10: 127.
9. Ma H, Zeng J, Realff ML, Kumar S, Schiraldi DA (2003) Comp Sci Technol 63:1617.
10. Legras R, Dekonick JM, Vanzieleghem A, Mercier JP, Nield E (1986) Polymer 27: 109.
11. Jawhari T, Roid A, Casado J (1995) Carbon 33: 1561.
12. Pantea D, Darmstadt H, Kaliaguine S, Summchen L, Roy C (2001) Carbon 39: 1147.
13. Takada T, Nakahara M, Kumagai H, Sanada Y (1996) Carbon 34: 1087.
14. Huang JC (2002) Adv Polym Technol 21: 299.
15. Wycisk R, Pozniak R, Pasternak A (2002) J Electrostatics 56: 55.

16. Yu G., Zhang M, Zeng H (1998) J Appl Polym Sci 70: 559.
17. Bueche F (1973) J Appl Phys 44: 532.
18. Meyer J (1973) Polym Eng Sci 13: 462.
19. Meyer J (1974) Polym Eng Sci 14: 706.
20. Narkis M, Ram A, Flashner F (1978) Polym Eng Sci 18: 649.
21. Mucha M, Marszalek J, Fidrych.A (2000) Polymer 41: 4137.
22. Mucha M, Krolikowski Z (2003) J Therm Anal Cal 74: 549.
23. Wiemann K, Kaminsky W, Gojny FH, Schulte K (2005) Macromol Chem Phys 206:1472.
24. Del Ria C, Ojeda MC, Acosta JL (2000) Eur Polym J 36: 1687.
25. Kim D, Seo K, Hong K, Kim S (1999) Polym Eng Sci 39: 500.
26. Fechine GJM, Rabello MS, Souto-Maior RM (2002) Polym Degrad Stab 75: 153.
27. Wu C, Zhou X, Zhang X, Xu H, Li H, Li X, Zhang L (2004) Chin Pat CN1781999.
28. Hess WM, Herd CR, Donnet J-B, Bansal RC, Wang M. (1993) Carbon Black Science and Technology. 2nd ed.,Marcel Dekker, New York.
29. Gopakumar TG, Lee JA, Kontopoulou M, Parent JS (2002) Polymer 43: 5483.
30. Cebe P, Hong S (1986) Polymer 27: 1183.
31. Avrami M (1940) J Chem Phys 8: 212.
32. Jeziorny A (1978) Polymer 19:1142.
33. Wan T, Chen L, Chua YC, Lu X (2004) J Appl Polym Sci 94: 1381.
34. Wan W, Chen G, Wu D (2003) Polymer 44: 8119.
35. Bian J, Ye S, Feng L (2003) J Polym Sci Part B 41: 2135.
36. Chae D W, Kim B C (2007) J Mater Sci 42:1238.
37. Jun YK, Park HS, Kim SH (2006) Polymer 47:1379. [35]
38. Lee C H, Saito H, Inoue T (1993) Macromolecules 26: 6566.
39. Ozawa T (1971) Polymer 12: 150. [36]
40. Liu T, Mo Z, Wang S, Zhang H (1997) Polym Eng Sci 37: 568.
41. Qiu Z, Mo Z, Yu Y, Zhang H, Sheng S, Song C (2000) J Appl Polym Sci 77: 2865.
42. Xu W, Ge M, He P (2001) J Appl Polym Sci 82: 2281.
43. Cebe P (1988) Polym Comp 9: 271.
44. Kissinger HE (1956) J Res Natl Bur Stand 57: 217.
45. Vyazovkin S (2002) Macromol. Rapid Commun. 23: 771.
46. Friedman H. (1964-1965) J Polym Sci Part C 6: 183.
47. Vyazovkin S (2001) J Comput Chem 22: 178.
48. Supaphol P, Dangseeyun N, Srimoaon P (2004) Polym Test 23: 175.